DOSAGE MEASUREMENTS USING ORGANIC SCINTILLATORS

ROBERT TURNER CARR

1953

Thesis
C2715

Library
U. S. Naval Postgraduate School
Monterey, California

M-49

DOSAGE MEASUREMENTS USING ORGANIC SCINTILLATORS

by

ROBERT TURNER CARR
B. S., U. S. Naval Academy
(1943)

SUBMITTED IN PARTIAL FULFILLMENT OF THE
REQUIREMENTS FOR THE DEGREE OF
MASTER OF SCIENCE

at the

MASSACHUSETTS INSTITUTE OF TECHNOLOGY
(1953)

Signature of Author...
Department of Physics, May 25, 1953

Certified by...
Thesis Supervisor

....
Chairman, Departmental Committee on Graduate Students

Library
U. S. Naval Postgraduate School
Monterey, California

Thesis
C2115

DUDLEY KNOX LIBRARY
NAVAL POSTGRADUATE SCHOOL
MONTEREY, CALIFORNIA 93940

ABSTRACT

Title: "Dosage Measurements Using Organic Scintillators"

Author: Robert Turner Carr

Submitted to the Department of Physics on May 25, 1953 in partial fulfillment of the requirements for the degree of Master of Science.

20655

An investigation, both theoretical and experimental, is made of the use of organic scintillators for dosage measurements. The "air-equivalent" range of organic scintillators is measured experimentally and found to be in close agreement with theory. Consideration of the following factors is taken into account:

1. Absorption in scintillator.
2. Size of scintillator.
3. Electronic equilibrium conditions.
4. Multiple scattering in scintillator.
5. External scattered radiation.

Measurements were made for several types and sizes of organic scintillators under both "good" geometry and "broad beam" geometry conditions. The conclusion is reached that under certain restricting conditions organic scintillators can be used for dosage measurements over a specified energy range of the incident γ radiation.

Thesis Supervisor: Robley D. Evans

Title: Professor of Physics

ACKNOWLEDGMENTS

The author wishes to express his appreciation to Dr. R. D. Evans, the thesis supervisor, for his advice and encouragement. Gratitude is also expressed to Dr. Gerald Hine who suggested the problem and aided the author materially during his investigations. Many thanks are also extended to all the personnel of the Radioactivity Center at M.I.T. where the thesis was performed. I am indebted to my wife for her patience and understanding during my period of research.

TABLE OF CONTENTS

Section I. Introduction and Statement of Problem 1
Section II. Theoretical Aspects 3
A. Basic Considerations 3
B. Energy Absorbed in γ-ray Interactions . . 5
C. Multiple Scattering 20
D. Electron Leakage 21
Section III. Experimental Equipment and Procedure . . 23
A. Ion Chamber Dosimeter 23
B. The Scintillation Dosimeter 24
C. Arrangement 25
Section IV. Experimental Results 28
A. "Good" Geometry 28
B. "Broad Beam" Geometry 36
Section V. Summary and Recommendations 46
A. Summary 46
B. Recommendations 48
C. Conclusion 49
Appendix A. Sample Calculations 51
Bibliography 56

LIST OF FIGURES

Number	Title	Page
1	γ-ray Mass Attenuation Coefficients for Air	7
2	γ-ray Mass Attenuation Coefficients for Anthracene	8
3	γ-ray Mass Attenuation Coefficients for NaI	9
4	Theoretical Ratio of Energy Absorbed/sec in Anthracene to Energy Absorbed/sec in Air vs E_γ	16
5	Theoretical Ratio of Energy Absorbed/sec in NaI to Energy Absorbed/sec in Air vs E_γ	19
6	Experimental and Theoretical Ratio of Energy Absorbed/sec in Anthracene to Energy Absorbed/sec in Air vs $\overline{E_\gamma}$	29
7	Comparison with Theoretical Ratio of Brucker's Experimental Results for Ratio of Energy Absorbed/sec in Anthracene to Energy Absorbed/sec in Air for X-ray Energies.	31
8	Dose Rate vs Wall Thickness for Air Ionization Chamber	33

9 Dose Rate vs Wall Thickness for 6 mm Anthracene Crystal 35

10 Experimental Ratio of Plastic Scintillator Response to Air Response vs Thickness of Plastic Scintillator 37

11 Ion Chamber Output vs Wall Thickness for Different Sources 39

12 Ion Chamber Output vs Wall Thickness for Different Source Distances 41

13 Experimental Ratio of Energy Absorbed/sec in Organic Scintillator to Energy Absorbed/sec in Air for Several Different Types and Sizes of Scintillators 43

14 Experimental and Theoretical Ratio of Energy Absorbed/sec in a NaI Crystal to Energy Absorbed/sec in Air 45

I. INTRODUCTION AND STATEMENT OF PROBLEM

There is a need in biological γ-ray studies for an instrument capable of measuring low dose rates. There are two requirements which such an instrument should meet. These are: (1) ability to measure dose rates in mr/hr (milliroentgens per hour) and (2) dimensions small enough such that the position of the detector for the γ radiation can be determined within a few millimeters.

The first requirement is necessary for an instantaneous knowledge of the dose rate. The second requirement would enable measurements of a radiation field with a high gradient or the determination of dose rates in intercavity measurements.

None of the instruments presently available meet both these requirements. The thimble chamber, which has small dimensions, is calibrated to read total roentgen dose and requires an excessive exposure time for small dose rates. Air ionization chamber dosimeters capable of reading low dose rates in mr/hr, are limited in their use because they require a relatively large ionization chamber.

An instrument capable of meeting both requirements has been proposed and investigated experimentally by

several authors(1, 2, 3). Such an instrument would be composed of an organic scintillator, a photomultiplier tube, and an electronic detecting system. In the first two papers(1, 2) which investigated the usefulness of this device over the low energy region (20 Kev-200 Kev), the detecting system merely measured the average direct current output of the photomultiplier tube by means of a direct current amplifier. Prestwich and Colvin(3) investigated a system for use in the medium energy γ-ray range (250 Kev-3 Mev), where the detecting system consisted of a highly complicated electronic spectrometer which they admit would be unsuitable for a practicable dose rate meter.

Dr. Gerald J. Hine suggested to the present author that the technique, as used by Ittner and Ter-Pogossian(1) of measuring directly the output of the photomultiplier tube should also be applicable to the medium energy range. Therefore the present author has undertaken an experimental investigation of such a system in the 250 Kev to 3 Mev range and this paper is a report of the investigation.

II. THEORETICAL ASPECTS

A. Basic Considerations

In radiobiology, radiation dose is measured in roentgens and dose rate in roentgens per unit time. The roentgen, as defined by the Radiological Congress at Chicago in 1937, is a unit of energy dissipation, or quantity of ionization, by γ or x-rays in a standard arbitrary material, air.(4) Therefore in order to measure the energy dissipation or quantity of ionization in roentgen units, the interacting material must either be air or a material "equivalent" to air. By "air-equivalent" material is meant a material in which the energy dissipated per gram of material is equal to the energy dissipated per gram of air.

To determine the energy dissipated in any material when there is an incident γ-ray flux, it is necessary to consider the detailed processes by which γ rays interact with matter. There are three main processes which have a probability of occurring when γ rays are incident on matter. These are (1) photoelectric effect, (2) Compton collisions, and (3) pair production. In the first two

processes the γ-ray photons interact with the electrons in matter and deliver part or all of their energy to an electron. This secondary electron then moves through the matter losing its kinetic energy, which it received from the incident γ-ray photon, by the process of ionization and excitation until all its energy is lost. In the third process the γ-ray photon is transformed in the field of a nucleus into a positron-electron pair both of which proceed to lose their energy in the same manner. The positron after losing its kinetic energy will react with another electron and produce annihilation radiation returning an energy of 1.02 Mev in the form of two γ rays each having an energy of 0.51 Mev.

Since the energy required for the production of an ion pair is roughly constant at about 32.5 ev/ion pair(5,6) the number of ion pairs is proportional to the energy delivered to the secondary electrons. This is the basis for the air ionization chamber which collects the ion pairs, measures their total charge, and obtains a measure of dosage.

In a scintillation crystal, light pulses are produced by a complicated scintillation process(7)

associated with the loss of energy through ionization. Hopkins(8) has shown that the light pulse in anthracene is proportional to the secondary electron energy initiating it at least for electron energies from 0.125 to 3.2 Mev. Since the photomultiplier current is proportional to the incident light flux the integrated current resulting from the scintillation pulses is a measure of the secondary electron energy or the energy dissipated in the crystal. This is the basis for a scintillation dose rate meter when the scintillation material is "air-equivalent".

B. Energy Absorbed in γ-ray Interactions

If the scintillation material is "air-equivalent" the ratio of the energy absorbed/sec in an organic scintillator to that absorbed/sec in air should be constant. To find this ratio we proceed as follows:

Let E_γ = γ-ray energy in Mev

E_γ^* = scattered γ-ray energy in Compton collision

n = number of incident photons/cm^2-sec of energy E_γ

A = effective area of incidence

σ = total Compton linear attenuation coefficient in cm^{-1}

$\sigma = \sigma_s + \sigma_a$

σ_a = true Compton linear absorption coefficient in cm^{-1}

σ_s = Compton scattering coefficient in cm^{-1}

τ = photoelectric linear attenuation coefficient in cm^{-1}

κ = pair production linear attenuation coefficient in cm^{-1}

μ_o = total linear attenuation coefficient in cm^{-1}

$\mu_o = \sigma + \kappa + \tau$

μ_a = true linear absorption coefficient in cm^{-1}

$\mu_a = \sigma_a + \kappa + \tau$

W = binding energy of "K" electron

Mass absorption coefficients are obtained by dividing the linear absorption coefficients by the density ρ. Figure 1 shows the value of μ/ρ, μ_a/ρ, τ/ρ, and κ/ρ for air as a function of incident γ-ray energy. Figure 2 is the same for anthracene and Fig. 3 is the same for NaI (see Appendix A for sample calculations and source of data).

In a Compton collision the energy absorbed per interacting photon is $(E_\gamma - E_\gamma^*)$ and the probability of

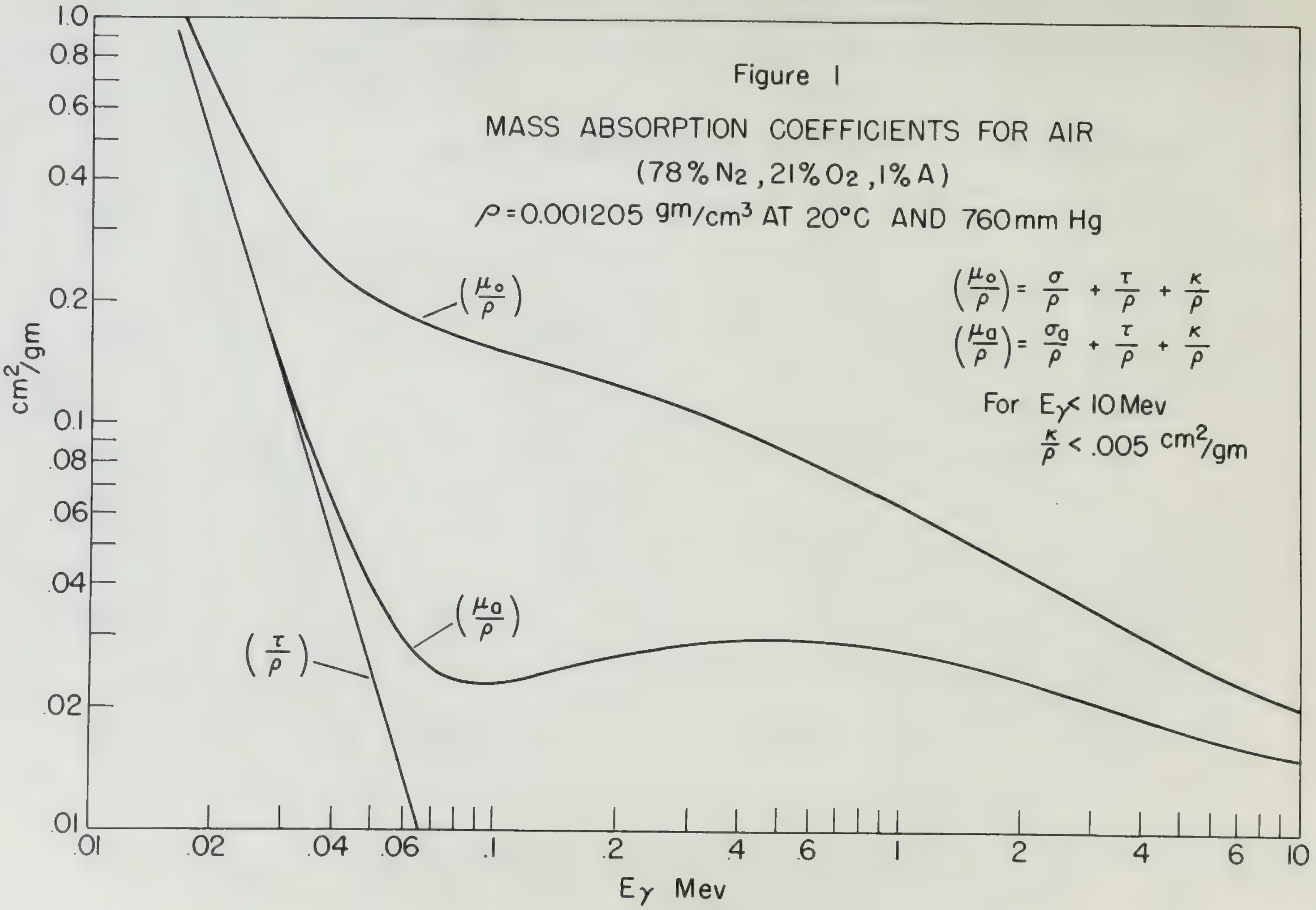

Figure 1

MASS ABSORPTION COEFFICIENTS FOR AIR

($78\% N_2$, $21\% O_2$, $1\% A$)

$\rho = 0.001205$ gm/cm^3 AT 20°C AND 760 mm Hg

$$\left(\frac{\mu_o}{\rho}\right) = \frac{\sigma}{\rho} + \frac{\tau}{\rho} + \frac{\kappa}{\rho}$$

$$\left(\frac{\mu_a}{\rho}\right) = \frac{\sigma_a}{\rho} + \frac{\tau}{\rho} + \frac{\kappa}{\rho}$$

For $E_\gamma < 10$ Mev

$\frac{\kappa}{\rho} < .005$ cm^2/gm

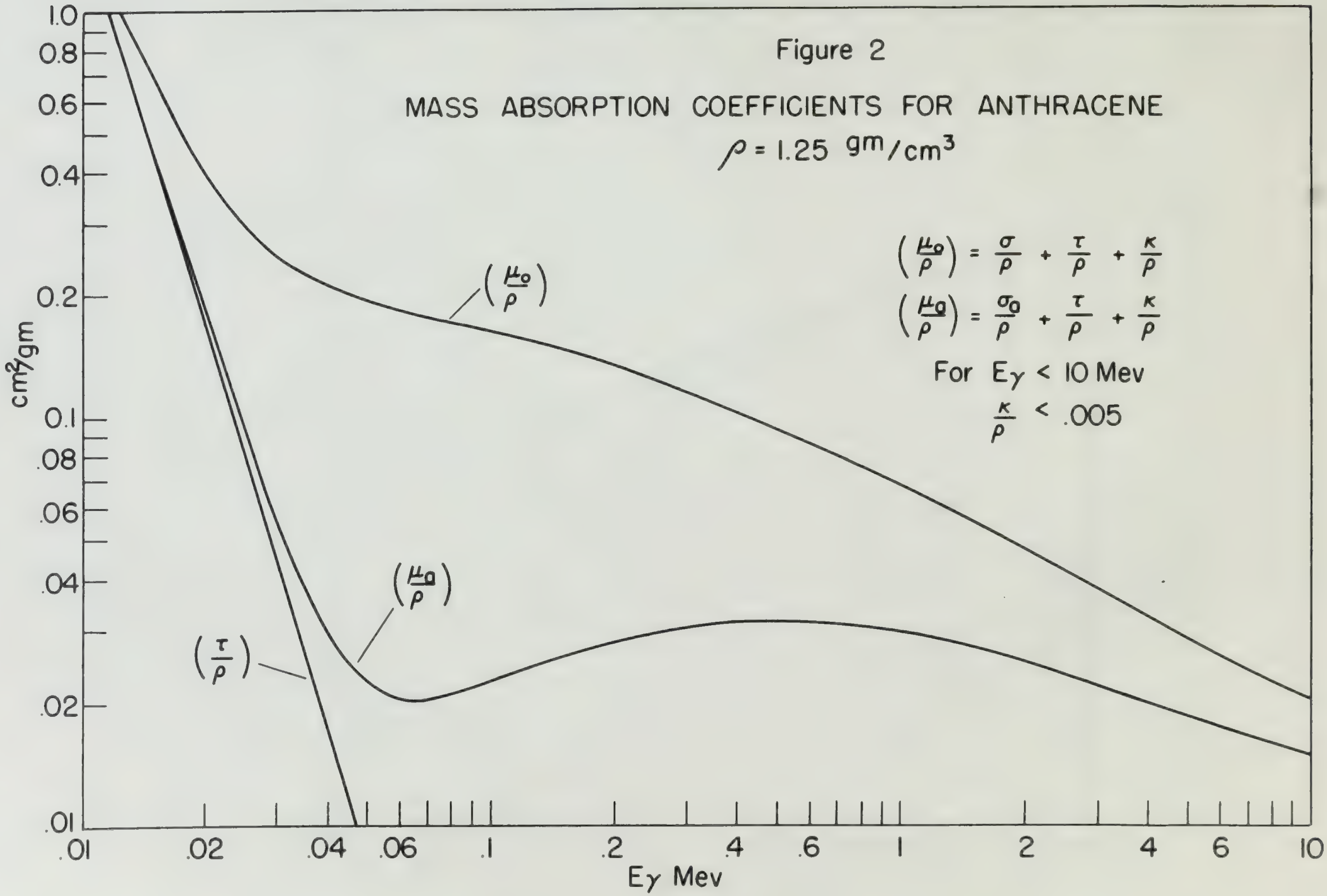

Figure 2

MASS ABSORPTION COEFFICIENTS FOR ANTHRACENE

$\rho = 1.25\ \mathrm{gm/cm^3}$

$$\left(\frac{\mu_o}{\rho}\right) = \frac{\sigma}{\rho} + \frac{\tau}{\rho} + \frac{\kappa}{\rho}$$

$$\left(\frac{\mu_a}{\rho}\right) = \frac{\sigma_a}{\rho} + \frac{\tau}{\rho} + \frac{\kappa}{\rho}$$

For $E_\gamma < 10$ Mev

$\frac{\kappa}{\rho} < .005$

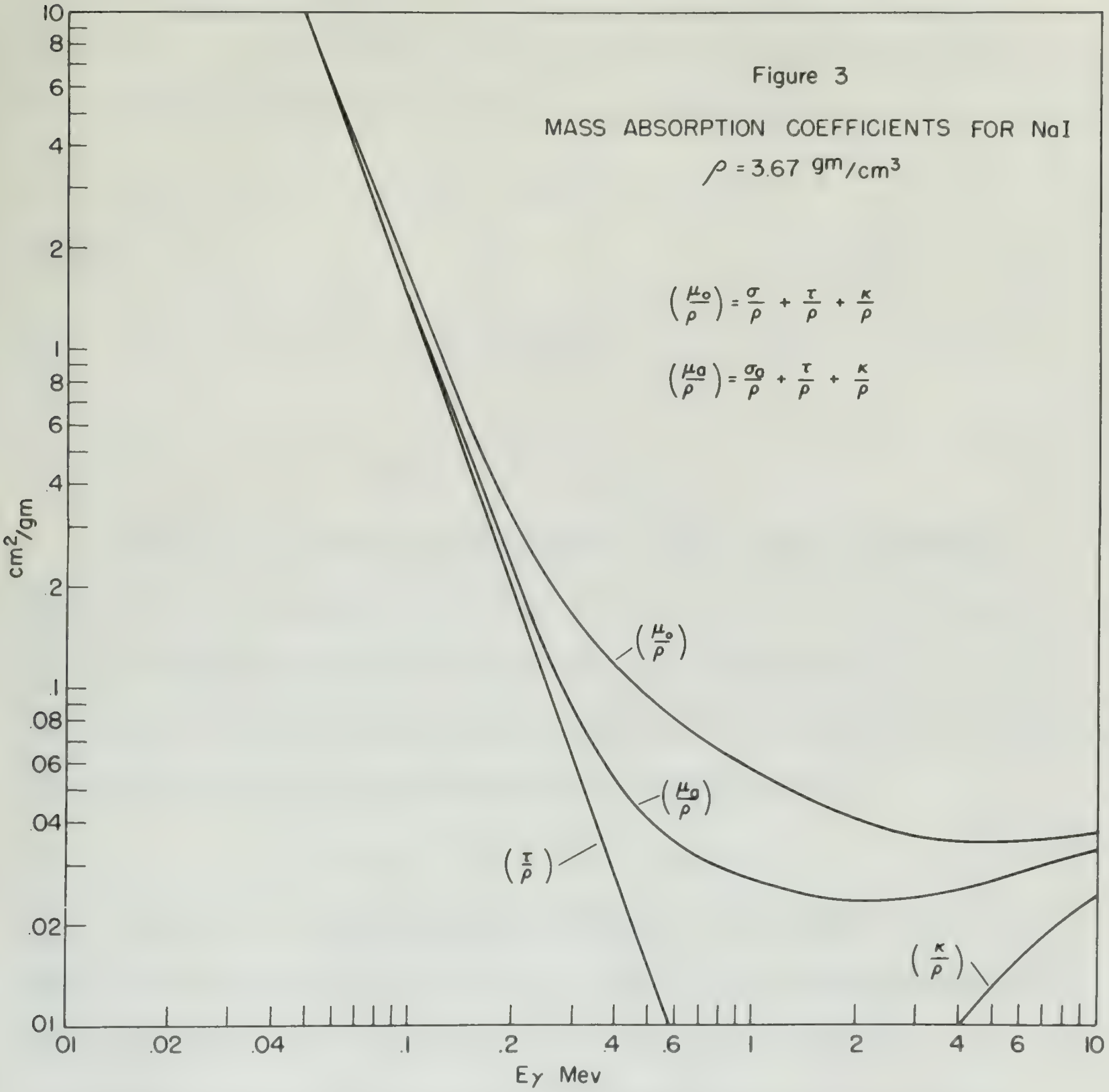

Figure 3

MASS ABSORPTION COEFFICIENTS FOR NaI

$\rho = 3.67\ \mathrm{gm/cm^3}$

$$\left(\frac{\mu_o}{\rho}\right) = \frac{\sigma}{\rho} + \frac{\tau}{\rho} + \frac{\kappa}{\rho}$$

$$\left(\frac{\mu_a}{\rho}\right) = \frac{\sigma_a}{\rho} + \frac{\tau}{\rho} + \frac{\kappa}{\rho}$$

interacting per photon per cm of path length is σ. Therefore the probable energy absorption per photon per cm of path length for a Compton collision is

$$\sigma(E_\gamma - E_\gamma^*)$$

Since

$$\sigma_a = \left(\frac{E_\gamma - E_\gamma^*}{E_\gamma}\right)\sigma$$

$$\sigma(E_\gamma - E_\gamma^*) = \sigma_a E_\gamma$$

In the photoelectric process the energy absorbed per interacting photon is $(E_\gamma - W)$ and the probability of interacting per photon per cm of path length is τ. Therefore the probable energy absorbed per photon per cm of path length in the photoelectric process is

$$\tau(E_\gamma - W)$$

In the pair-production process the energy absorbed per interacting photon is $(E_\gamma - 2m_0c^2)$ and the probability of interacting per photon per cm of path length is κ. Therefore the probable energy absorbed per photon per cm of path length in the pair-production process is

$$\kappa(E_\gamma - 2m_0c^2)$$

The total probable energy absorbed per sec = dE_T for an incident flux of n photons/cm^2-sec in a thickness = dx is the sum of the probable energies absorbed per unit time in a thickness dx for the three processes.

$$dE_T = nA\left[dx \quad \sigma_a E_\gamma + \quad (E_\gamma - W) + \quad (E_\gamma - 2m_oc^2)\right] \qquad \text{(B-1)}$$

The total energy per sec absorbed in a thickness ℓ is

$$E_T = \int_o^{\ell} dE_T \qquad \text{(B-2)}$$

For air and organic materials, in the energy range considered (0.01 Mev to 10 Mev), W is negligible compared to E_γ. Also since $\kappa(E_\gamma - 2m_oc^2) \ll \sigma_a E_\gamma$ this term can be neglected. Using these simplifying assumptions the equation for energy absorbed per sec in dx becomes

$$dE_T = nAE_\gamma(\sigma_a + \tau)\ dx = nAE_\gamma \mu_a\ dx \qquad \text{(B-3)}$$

In a material whose thickness is ℓ, the number of photons/cm^2-sec, n, incident on a cross section taken anywhere between 0 and ℓ is not constant but follows an exponential law

$$n = n_o e^{-\mu_o x} \qquad \text{(B-4)}$$

The total linear attenuation coefficient μ_o is chosen here on the basis of crystal size, which makes the

probability of multiple scattering extremely unlikely. The actual value lies somewhere between μ_a and μ and is dependent on the geometry.(5) The total energy absorbed per sec then becomes

$$E_T = \int_0^{\ell} n_o e^{-\mu_o x} A E_\gamma \mu_a \, dx$$

$$= n_o \mu_a E_\gamma \ell A \left[\frac{1 - e^{-\mu_o \ell}}{\mu_o \ell} \right] \qquad \text{(B-5)}$$

Using primed symbols to indicate values for air and unprimed symbols for organic scintillators the ratio of energy absorbed per sec in an organic scintillator to the energy absorbed per sec in air becomes

$$R = \frac{n_o \mu_a E_\gamma \ell A \left[\frac{1 - e^{-\mu_o \ell}}{\mu_o \ell} \right]}{n_o \mu_a' E_\gamma \ell' A' \left[\frac{1 - e^{-\mu_o' \ell'}}{\mu_o' \ell'} \right]} \qquad \text{(B-6)}$$

For an ionization chamber of reasonable size (1-2 liter volume, 3-4 mm air equivalent wall material) $\mu_o' \ell' \ll 1$, therefore $1 - e^{-\mu_o' \ell'} \cong \mu_o' \ell'$ and the ratio becomes

$$R = \frac{\mu_a}{\mu_a'} \frac{\ell A}{\ell' A'} \frac{1 - e^{-\mu_o \ell}}{\mu_o \ell} \qquad (B\text{-}7)$$

For a specified organic scintillator and ion chamber the ratio $\frac{\ell A}{\ell' A'}$ will remain constant. The ratio R can then be written

$$R = C \frac{\mu_a}{\mu_a'} \frac{1 - e^{-\mu_o \ell}}{\mu_o \ell} \qquad (B\text{-}8)$$

Since we are interested only in the relative values of R the value of the constant C can be chosen to normalize R to one at any selected value of E_γ. Note that this ratio is a function of crystal thickness.

All of the above equations have been derived on the assumption of a monoenergetic γ-ray source. We must investigate the problem also for non-monoenergetic sources.

First we define an average γ-ray energy

$$\overline{E_\gamma} = \sum_i P_i E_{\gamma_i} / \sum P_i$$

where

P_i = percent abundance of i'th γ ray

E_{γ_i} = energy of i'th γ ray

then
$$dE_{T_i} = n_i A E_{\gamma_i} \mu_{a_i}\, dx \qquad \text{(B-10)}$$

$$dE_T = \sum_i n_i A E_{\gamma_i} \mu_{a_i}\, dx \qquad \text{(B-11)}$$

$$n_i = n_{o_i} e^{-\mu_{o_i} x} \qquad \text{(B-12)}$$

$$E_T = \int_o^{\ell} \sum n_{o_i} e^{-\mu_{o_i} x} A E_{\gamma_i} \mu_{a_i}\, dx$$

$$= \sum_i n_{o_i} \mu_{a_i} E_{\gamma_i} A \ell \left[\frac{1 - e^{-\mu_{a_i} \ell}}{\mu_{a_i} \ell} \right] \qquad \text{(B-13)}$$

Using the expansion for $e^{-\mu_o' \ell'}$ for air, as before, the ratio of energy absorbed per sec by the organic scintillator to energy absorbed per sec by air becomes

$$R = \frac{C \sum_i n_{o_i} \mu_{a_i} E_{\gamma_i} \left[\frac{1 - e^{-\mu_{o_i} \ell}}{\mu_{o_i} \ell} \right]}{\sum_i n_{o_i} \mu_{a'_i} E_{\gamma_i}} \qquad \text{(B-14)}$$

For the sources used experimentally which have a non-monoenergetic spectrum the greatest correction (not considering Ra) will occur for the Na^{24} source which has two γ rays of widely divergent energy. Calculation of the ratio R, considering the separate γ rays, compared with

the calculation of R, considering the source monoenergetic with a γ-ray energy equal to the average γ-ray energy of Na^{24}, shows that this correction is less than 1 percent (see Appendix A). We therefore conclude that if we consider all our sources monoenergetic with an energy equal to their average γ-ray energy as defined in equation (B-9) no appreciable error will be introduced.

In Fig. 4 are shown the theoretical results of the calculation of the ratio R for anthracene crystals of different thickness. The curve drawn for a crystal thickness of 0 mm is obtained from equation (B-8) by setting the thickness correction factor $\left[\frac{1 - e^{-\mu_0 \ell}}{\mu_0 \ell}\right] = 1$. This is equivalent to the assumption that there is no loss due to absorption of primary radiation in a crystal whose thickness is ℓ, (i.e., $n = n_0$ in equation (B-4)). The value of the constant C is chosen so that the computed ratio R for $E_\gamma = 0.6$ Mev is equal to 1. This value is chosen since the investigation of Fig. 2 shows that at 0.6 Mev τ/ρ and κ/ρ are very small compared with σ_a/ρ and therefore, at this energy, anthracene should be "air-equivalent". Figure 4 shows that the energy chosen for the normalization point could have been selected anywhere

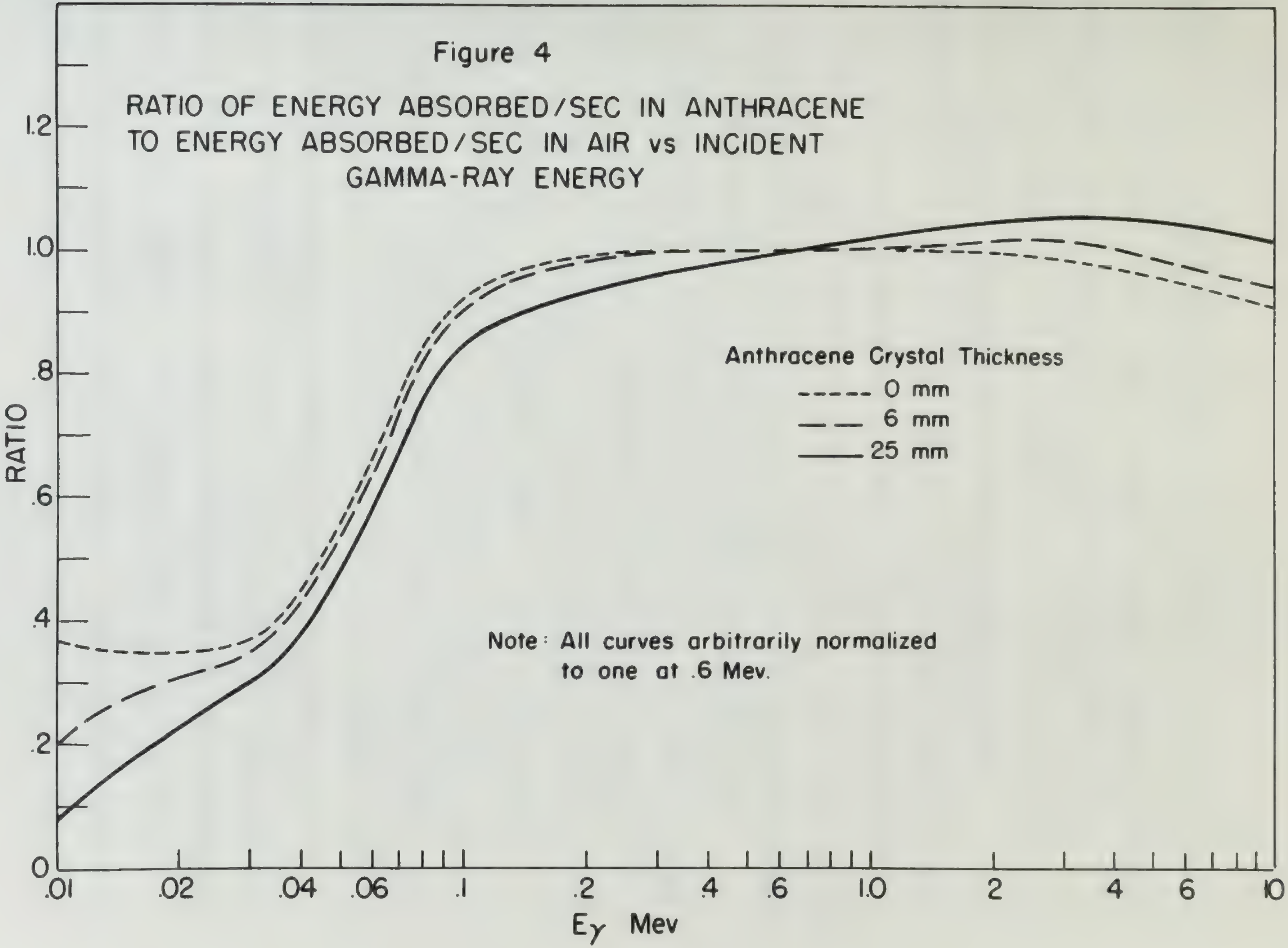

Figure 4

RATIO OF ENERGY ABSORBED/SEC IN ANTHRACENE TO ENERGY ABSORBED/SEC IN AIR vs INCIDENT GAMMA-RAY ENERGY

Note: All curves arbitrarily normalized to one at .6 Mev.

between 0.3 and 2.0 Mev since in this region the ratio is linear and equal to 1. This energy range is the true "air-equivalent" range under the assumption that there is no loss in the crystal due to absorption. Below 0.3 Mev the ratio is seen to decrease and this is caused by the difference between the photoelectric absorption coefficient, τ/ρ, for air and anthracene. Above 2.0 Mev the ratio is also observed to decrease and this is caused by the difference in pair production coefficients, κ/ρ, for the two materials.

By introduction of the correction factor we would expect the ratio to be greatly decreased in the lower energy range and only slightly decreased in the higher energy range since, for energies < 10 Mev, μ_0 increases as the energy decreases. The decrease should also be more pronounced as ℓ increases. Investigation of the curves for 6 mm thickness and 25 mm thickness in Fig. 4 shows that the decrease in ratio as a function of ℓ is as expected. The relative decrease as a function of energy is masked as a result of the choice of 0.6 Mev as the normalization energy. To show this effect the curves should be drawn with absolute values for the ratio R. The general shape of the curves remains the same as for the 0 mm case. However, the linear portion of the curve above 0.1 Mev no longer has 0 slope.

The choice of 0.6 Mev as the normalization energy is made since this energy lies at the middle of the linear portion of the curve and gives the greatest approximately "air-equivalent" range. The "air-equivalent" ranges witnin ± 5 percent are

Crystal thickness	"Air-equivalent" range ± 5 percent
0 mm	0.11 Mev - 6.0 Mev
6 mm	0.13 Mev - 9.0 Mev
25 mm	0.25 Mev - >10 Mev

In Fig. 5 the theoretical value of the ratio R as a function of energy is shown for a NaI crystal. The discussion given above for Fig. 4 is also applicable for this case. The normalization energy for NaI was selected as 1.5 Mev since investigation of Fig. 3 shows that τ/ρ and κ/ρ are very small compared to σ_a/ρ at this energy. Therefore at this energy NaI should be "air-equivalent". The approximate "air-equivalent" ranges within ± 5 percent for NaI are

Crystal thickness	"Air-equivalent" range ± 5 percent
0 mm	0.62 Mev - 3.3 Mev
25 mm	0.50 Mev - 3.0 Mev

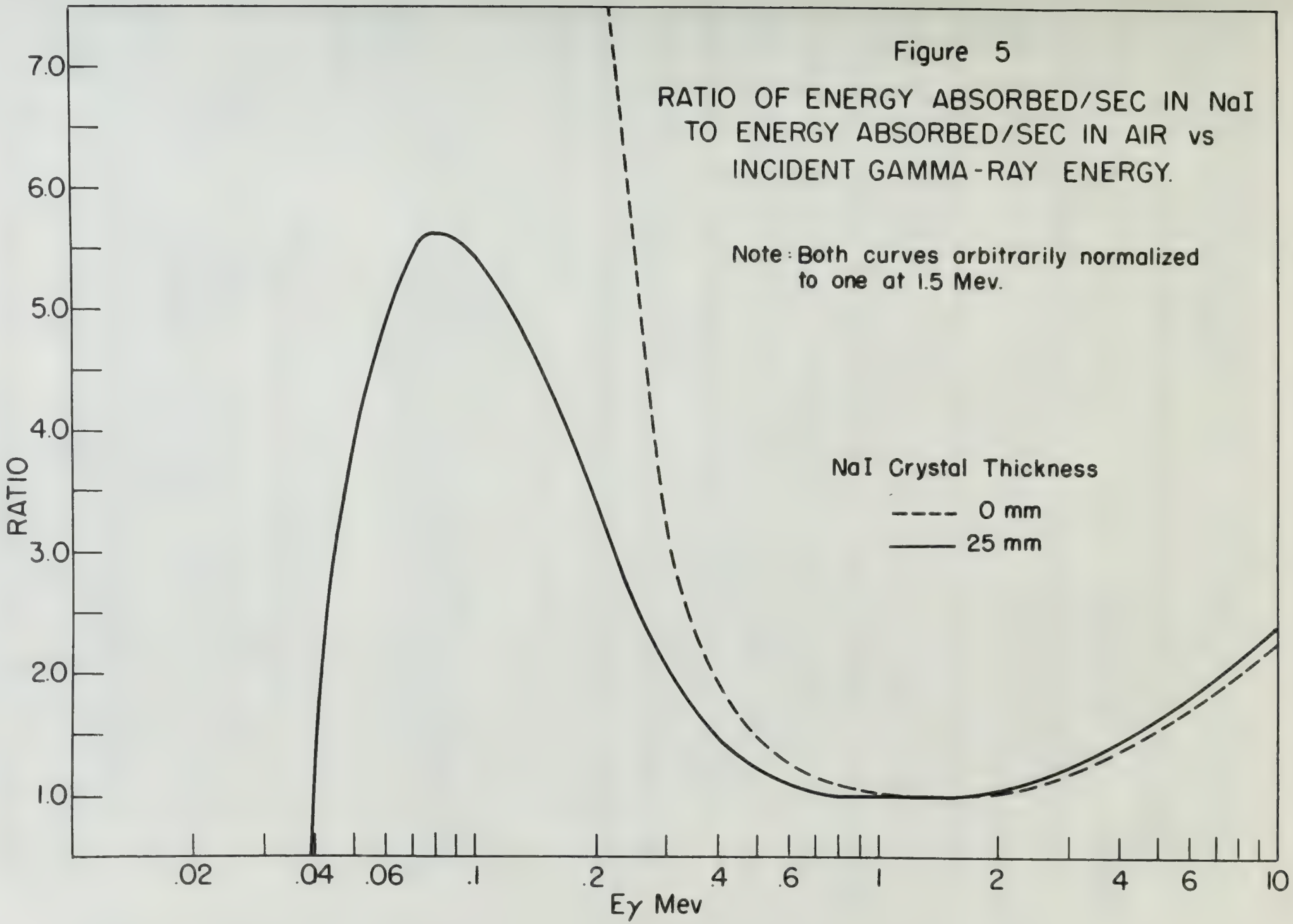

Figure 5

RATIO OF ENERGY ABSORBED/SEC IN NaI TO ENERGY ABSORBED/SEC IN AIR vs INCIDENT GAMMA-RAY ENERGY.

Note: Both curves arbitrarily normalized to one at 1.5 Mev.

C. Multiple Scattering

The effect of multiple scattering must be considered in this treatment of the theoretical aspects of the problem. Multiple scattering would be greatest for low energies and and for thick organic scintillators. Prestwich and Colvin$^{(3)}$ estimated, under gross assumptions, that in a 20 mm thick anthracene crystal at an incident γ-ray energy of 280 Kev a maximum value of 3.4 percent of the incident photons could suffer 2 collisions. Using this value and neglecting any multiple collisions in the ion chamber since $1/\mu_o \gg$ wall thickness of ion chamber, we can calculate a new ratio taking into account the energy absorbed in the crystal as a result of multiple collisions. Proceeding as before the ratio then becomes

$$R = \frac{n_o\mu_a E_\gamma \ell A\left[\frac{1 - e^{-\mu_o \ell}}{\mu_o \ell}\right] + 0.034 n_o \mu_a{}^{*}\overline{E_\gamma{}^{*}}\ell^{*}A\left[\frac{1 - e^{-\mu_o{}^{*}\ell^{*}}}{\mu_o{}^{*}\ell^{*}}\right]}{n_o\mu_a{}' E_\gamma \quad {}'A'}$$

where

$\overline{E_\gamma{}^{*}}$ = average energy of scattered γ rays

$\mu_a{}^{*}$ = true linear absorption coefficient for a γ-ray energy of $\overline{E_\gamma{}^{*}}$

$\mu_o{}^{*}$ = total linear attenuation coefficient for a γ-ray energy of $\overline{E_\gamma{}^{*}}$

ℓ^{*} = average path length in crystal for a scattered γ ray

Since $\overline{E_\gamma^*} = \frac{\sigma_s}{\sigma_s + \sigma_a} E_\gamma$ and for a cylindrical crystal whose diameter is equal to its length $\ell^* \cong \ell/2$ this ratio can be written

$$R = \frac{C\left\{\mu_a\left[\frac{1 - e^{-\mu_o \ell}}{\mu_o \ell}\right] + 0.017\mu_a^*\left(\frac{\sigma_s}{\sigma_s + \sigma_a}\right)\left[\frac{1 - e^{-\mu_o^* \ell^*}}{\mu_o^* \ell^*}\right]\right\}}{\mu_a'}$$

The percent increase in R when the effect of multiple scattering is considered is then

$$\text{percent increase in R} = \frac{1.7\mu_a^*\left(\frac{\sigma_s}{\sigma_s + \sigma_a}\right)\left[\frac{1 - e^{-\mu_o^* \ell^*}}{\mu_o^* \ell^*}\right]}{\mu_a\left[\frac{1 - e^{-\mu_o \ell}}{\mu_o \ell}\right]}$$

For a cylindrical anthracene crystal with a diameter and length equal to 20 mm, and an incident γ-ray energy of 280 Kev then the calculated percent increase in R is

$$\text{percent increase in R} = 1.2$$

We therefore conclude that under the conditions of this experiment the effect of multiple scattering will be negligible.

D. Electron Leakage

In concluding the theoretical aspect of the problem the effect of electron leakage will be considered. At high energies some of the secondary electrons produced in

the scintillator will have mean ranges which are comparable to the dimensions of the scintillator. This means that some of the electrons will escape from the surfaces of the scintillator before all their energy has been dissipated in the scintillator. The ratio of energy absorbed/sec in the scintillator to energy absorbed/sec in air will then be lower than that computed by theory. This difficulty should be removed if an "air-equivalent" material thick enough to provide electronic equilibrium surrounds the crystal. Electronic equilibrium will occur, when the thickness of the surrounding material is approximately equal to the maximum range of the secondary electrons in the material.(10) This will be investigated experimentally.

III. EXPERIMENTAL EQUIPMENT AND PROCEDURE

The equipment used in this experiment consisted of two basic measuring systems; (1) an air ionization dose rate meter and (2) a scintillation dose rate meter.

A. Ion Chamber Dosimeter

The air ionization chamber dose rate meter selected for use in this experiment was a commercial Beckman Radioactivity Meter, Model MX-4. The ionization chamber used with this meter is a 3 mm bakelite cylinder whose volume is approximately 1.6 liters. The ion chamber was always placed so that the source was on its axis and in this position the front cover of the ion chamber is removable leaving a thin celluloid window 0.10 inches thick. The ion chamber is connected to the meter by a coaxial cable approximately 6 feet long. The most sensitive scale on the meter has a full scale deflection of 1 mr/hr. The next scale has a full scale deflection of 2 mr/hr and the next scale which is the most stable of the lower three scales has a full scale deflection of 5 mr/hr. The source strength and distances were always chosen to give a reading on the 5 mr/hr scale. All readings taken were corrected for non-linearity of the scale with a maximum correction

for center scale readings of approximately 1 percent of full scale deflection.

B. The Scintillation Dosimeter

The scintillation dosimeter consisted of one of several types of organic scintillators mounted on an RCA 5819 photomultiplier tube. The photomultiplier was always operated at a negative voltage of 750 volts. The output of the photomultiplier was connected directly to a modified RCA WV-84A DC microammeter. The modification consisted of inserting a feedback capacitance of 1.0 μf between the plate and grid of the input tube. This is essentially the same arrangement as used by Ittner and Ter-Pogossian.(1) The purpose of the feedback capacitance is to smooth out the input which is in a series of pulses from the photomultiplier tube. Care must be exercised in the selection of the capacitor used in such a modification as a capacitor having only slight leakage will cause excessive drift in the meter. The meter used in this experiment had a drift of less than 1 percent of full scale deflection per hour on any scale.

All of the organic scintillators used in this experiment, with the exception of the 6 mm anthracene crystal which was cut to fit the top of the photomultiplier tube,

were mounted on a cylindrical lucite light pipe 3 mm thick and 37 mm in diameter cut to fit the top of the phototube. The sides and backs of all the scintillators were covered with 1/4 mil aluminum foil to increase the light collecting efficiency. Optical matching was obtained by the use of Nujol.

All measurements were made with a μ-metal shield around the phototube and a light cardboard shield was placed around the phototube and scintillator assembly to remove stray visible light.

C. Arrangement

In order to reduce to as small an extent as possible any contribution from scattered radiation the ion chamber and phototube scintillator assembly were mounted on a light aluminum frame approximately 2 meters apart and 1.3 meters above a wooden table. For "broad beam" geometry the sources were positioned between the two detectors, suspended from strings, at the same height above the table. The ceiling, walls, and floor were all at a distance greater than 2.5 meters from either detector or source.

Distances from source to detector for the scintillation arrangement were measured from center of source to center of crystal. For the ion chamber the distance was computed

using the formula(11)

$$x = \sqrt{a(\ell + a)}$$

where a = distance from front wall of ion chamber to center of source and ℓ = depth of ion chamber. The sources used are described in the table given below.

Source		$\underline{E}_\gamma$	$\underline{P}_1$	$\overline{E}_\gamma$
Hg^{203}	2 ml acid soln.	280 Kev	100 percent	280 Kev
I^{131}	2 ml acid soln.	Complex(12)		367 Kev
Cs^{137}	0.1 ml acid soln.	663 Kev	100 percent	663 Kev
Ra	Ra salt, 0.5 mm Pt filter	Complex		1.04 Kev(13)
Co^{60}	1/4" 15 mil wire	1.17 Mev	100 percent	1.25 Mev
		1.33 Mev	100 percent	
Na^{24}	3 gm Na_2CO_3	1.38 Mev	100 percent	2.07 Mev
		2.76 Mev	100 percent	

For the "broad beam" geometry the sources were enclosed in 5 ml glass vials, wall thickness 1 mm, except the Ra source which was enclosed in a 3/4 inch diameter solid lucite container.

For the "good" geometry the sources were placed in glass test tubes (13 mm diameter, 1 mm wall thickness) which were inserted in a lead collimator whose dimensions

are shown in the figure below.

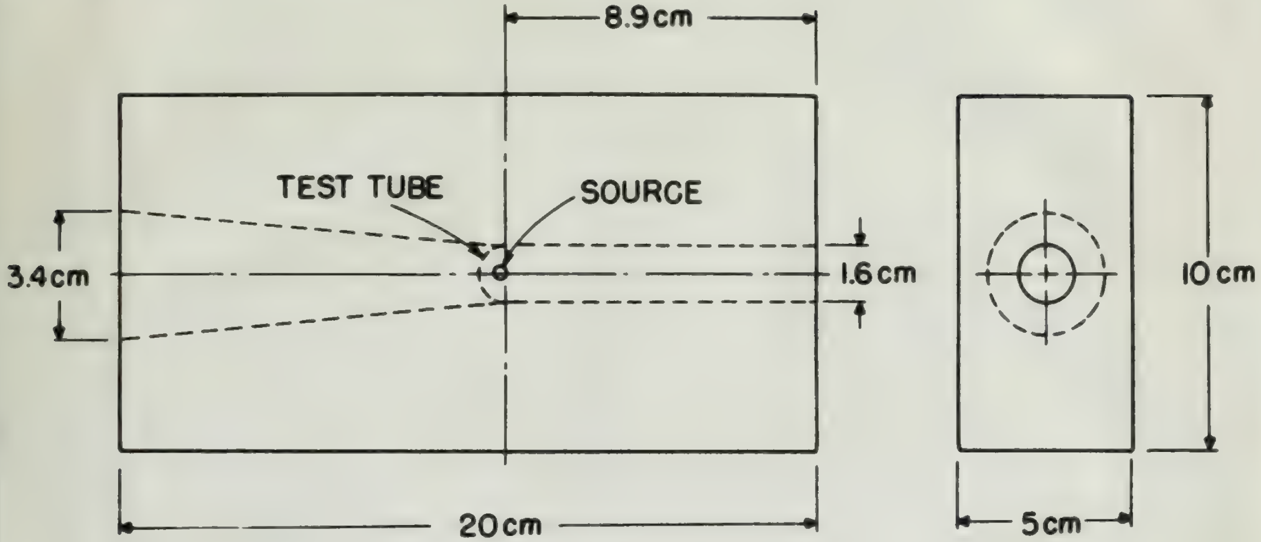

LEAD COLLIMATOR

A piece of bakelite 4 mm thick covered the exit port of the collimator to absorb the secondary electrons and fluorescent radiation emitted from the collimator. The collimator was positioned at the height of the detectors on a light aluminum framework.

IV. EXPERIMENTAL RESULTS

A. "Good" Geometry

The theory as outlined in Section II is based only on primary radiation. In order to check this theory it is therefore necessary to eliminate any possible effects that might occur as a result of scattered radiation. It was at first thought that by using the arrangement as described in Section III of placing the sources and detectors at least 2.5 meters from the walls, floor, and ceiling there would be negligible contributions from scattered radiation to the dose rate as measured at the detectors. Investigation, to be described in this section, proved this premise to be incorrect and led to the use of a collimated source and "good" geometry for the experimental measurements to be used for comparison with theory.

Figure 6 shows the experimental results obtained using a 6 mm anthracene scintillation crystal. The experimental points were normalized by comparison with the result obtained for Cs^{137} whose γ-ray energy is 663 Kev. For this energy the theoretical curve plotted in Fig. 6 and normalized at 600 Kev, also has a value of one. There is excellent agreement with theory using "good" geometry

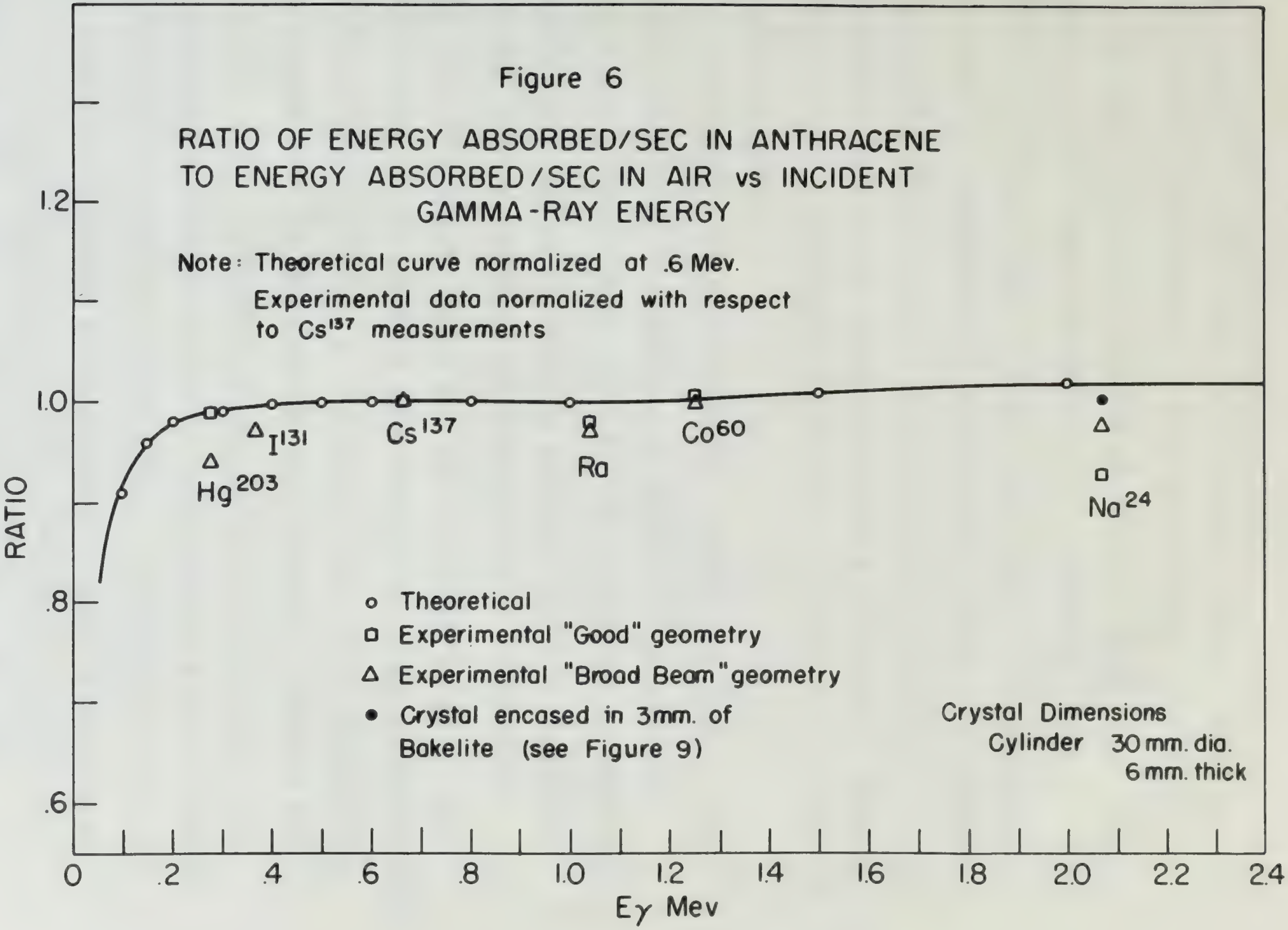

Figure 6

RATIO OF ENERGY ABSORBED/SEC IN ANTHRACENE TO ENERGY ABSORBED/SEC IN AIR vs INCIDENT GAMMA-RAY ENERGY

Note: Theoretical curve normalized at .6 Mev.
Experimental data normalized with respect to Cs^{137} measurements

for the Hg^{203}, Cs^{137}, and Co^{60} γ-rays. The low value for the Na^{24} measurement is believed to be a result of the electron leakage discussed in Section II-C. The result for Na^{24} when the crystal is encased in 3 mm of bakelite is also shown in Fig. 6 and the closer agreement to theory is attributed to the improved electronic equilibrium which exists under these conditions. Separate investigations of the leakage loss as a function of crystal thickness and equilibrium conditions are presented later in this section.

An attempt to correlate the results obtained in this energy range with the results of Brucker(2) in the low energy range is shown in Fig. 7. His experimental results, assuming his measured value at 185 Kev to be in agreement with the theory outlined in Section II, are shown along with the theoretical curve and the measured value of the Hg^{203} source, used in this experiment, for a 25 mm anthracene crystal. The results are considered quite good considering the uncertainty in the average x-ray energy. However the increased rate of fall-off at the lower energies could be a result of scattered radiation resulting in a lower average energy than that of the primary beam for which the energies are given. No mention of scattering is made in his paper.

In accordance with Gray's(5, 14) cavity theorem to obtain correct measurements with ionization chambers

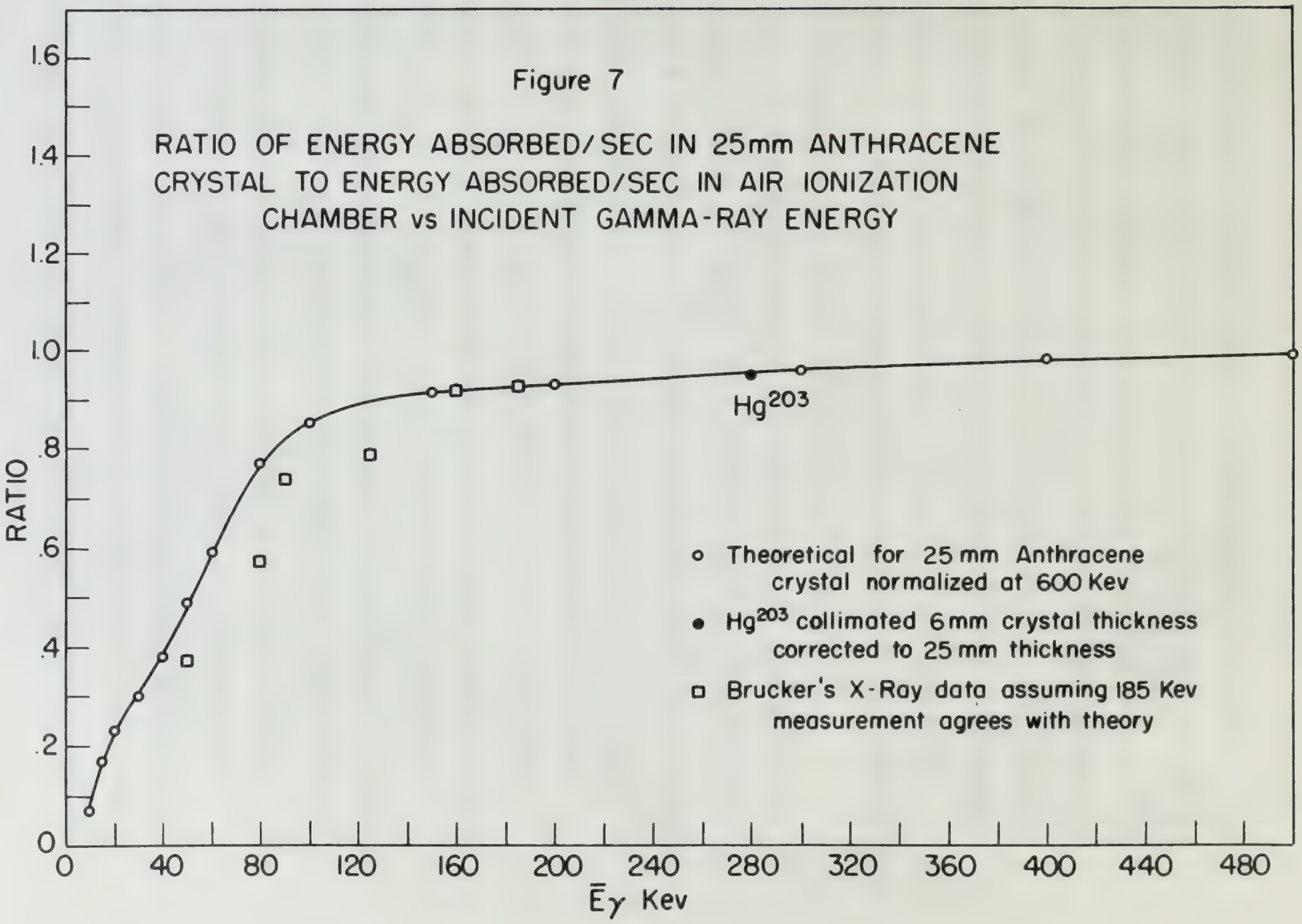

Figure 7

RATIO OF ENERGY ABSORBED/SEC IN 25mm ANTHRACENE CRYSTAL TO ENERGY ABSORBED/SEC IN AIR IONIZATION CHAMBER vs INCIDENT GAMMA-RAY ENERGY

(and the same principle can be extended to organic scintillators) there must be electronic equilibrium of the secondary electrons in the region in which the cavity or detecting medium is located. By electronic equilibrium is meant that the rate of flow of secondary electrons in a small differential volume is the same in one direction as in the opposite direction. In order to check the detecting instruments used in this experiment for equilibrium conditions the following measurements were made:

1. The front wall of the ion chamber was built up in steps using celluloid and bakelite and readings taken using a collimated Na^{24} source approximately 40 cm in front of the chamber. It was felt necessary to increase only the front wall thickness as Mayneord and Roberts(11) have stated that the largest contribution to the ionization inside the ion chamber arises from the front wall. The Na^{24} source was selected since equilibrium conditions require an increased wall thickness as the energy of the primary radiation increases, therefore the effect of non-equilibrium should be more pronounced for this source. The results, using a collimated source, are shown in Fig. 8, curve A, and the expected build-up in ionization as the equilibrium conditions are reached at 6 mm wall thickness is readily apparent. The other curves shown in

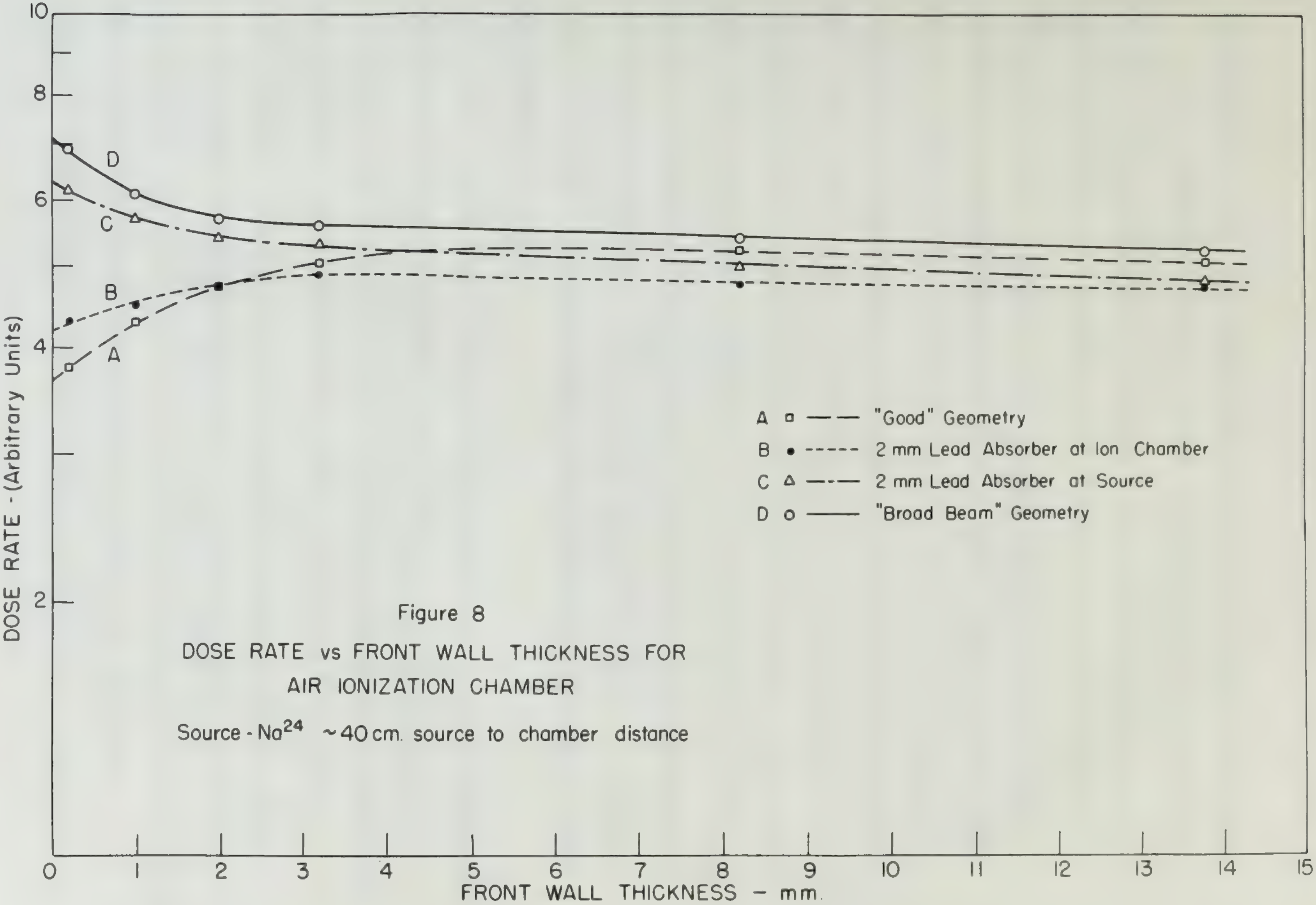

Figure 8

DOSE RATE vs FRONT WALL THICKNESS FOR AIR IONIZATION CHAMBER

Source - Na^{24} ~40 cm. source to chamber distance

this figure will be discussed in part B of this section.

2. Essentially the same experiment was performed on the 6 mm anthracene crystal. The crystal was encased in a cylinder of bakelite 6 mm thick and then different thickness front covers were placed over the crystal to check the equilibrium conditions. Two sources were used in this experiment, Na^{24} and Co^{60}. The results and diagram of the arrangement are shown in Fig. 9. For the Co^{60} source no build-up with wall thickness is observed leading to the conclusion that for this energy, 1.25 Mev, and this thickness of crystal, 6 mm, equilibrium conditions can be achieved in the crystal itself with zero thickness of encasing material. The curve for Na^{24} shows a definite build-up with a maximum when the front wall thickness is increased to 3 mm.

To obtain some idea of the leakage loss as a function of crystal size, a plastic scintillator was obtained from the Pilot Chemical Company of Waltham, Mass. The selection of a plastic scintillator was made as it can be easily machined and polished to any desired shape or size. The γ-ray attenuation coefficients for plastic are essentially the same as for anthracene. The original plastic scintillator was a cylinder 25 mm in height and 26 mm in diameter. Several scintillators of the same diameter but different

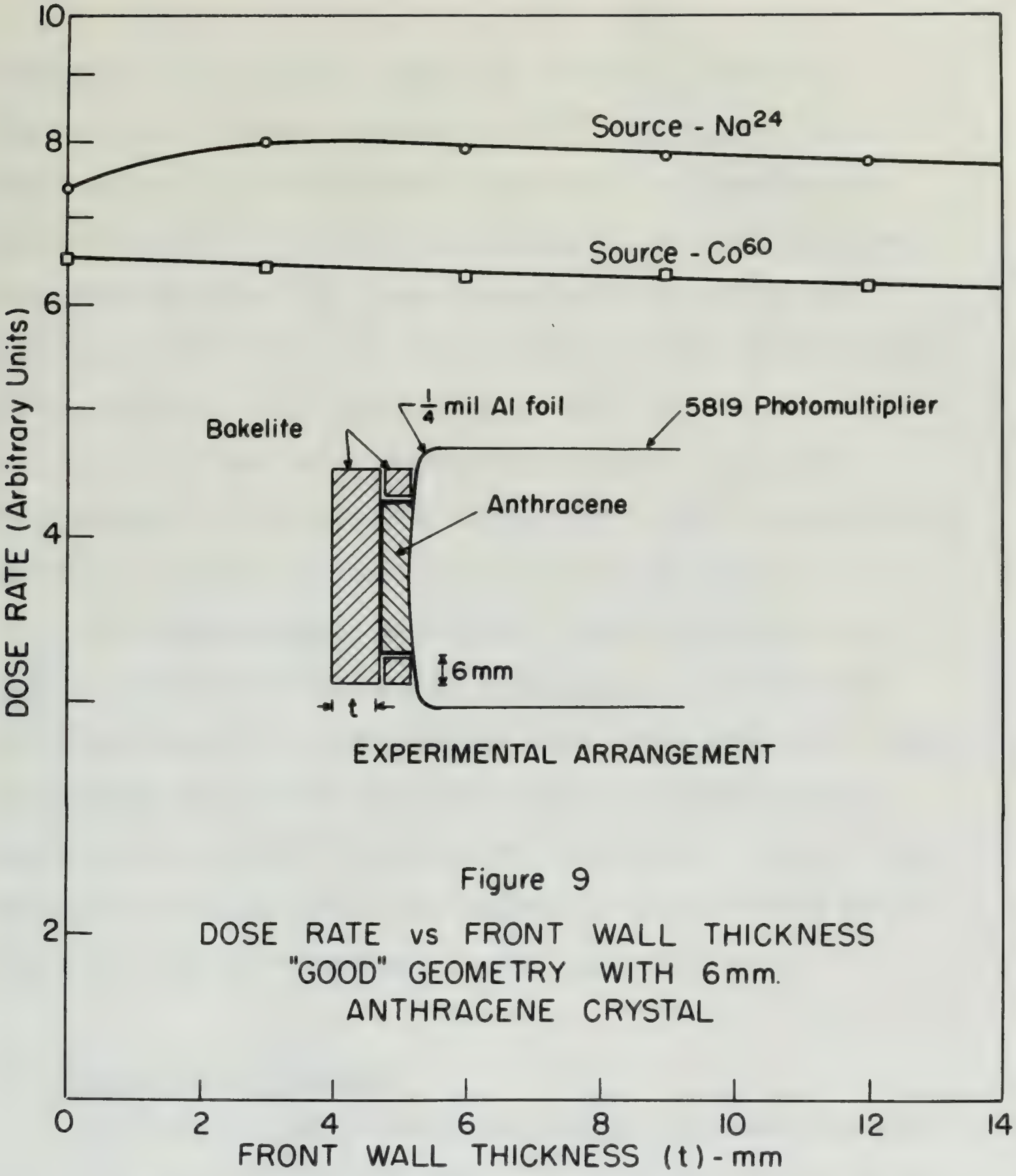

Figure 9

DOSE RATE vs FRONT WALL THICKNESS
"GOOD" GEOMETRY WITH 6 mm.
ANTHRACENE CRYSTAL

thickness were machined from the original cylinder. Measurements using a collimated Na^{24} source were made and the ratio of ion chamber response to scintillation meter response as a function of scintillation thickness are shown in Fig. 10. The ratios are plotted on the assumption that the loss for the 25 mm thick scintillator is negligible. The difference in dose rate as a result of absorption has been eliminated in this series of measurements by correlation with lower energy measurements and normalization at the average energy of Na^{24}.

The measurements made using "good" geometry are useful primarily in checking the theory. In practical applications of a scintillation dose rate meter for radiobiological work it is expected that most measurements would be made under "broad beam" conditions. Some of the effects caused by scattered radiation using "broad beam" geometry will be discussed in the next section.

B. "Broad Beam" Geometry

When using "broad beam" geometry many new variables are introduced into the problem. No attempt will be made in this discussion to investigate these different variables but the main effects of scattered radiation on dosage measurements when using organic scintillators will be presented.

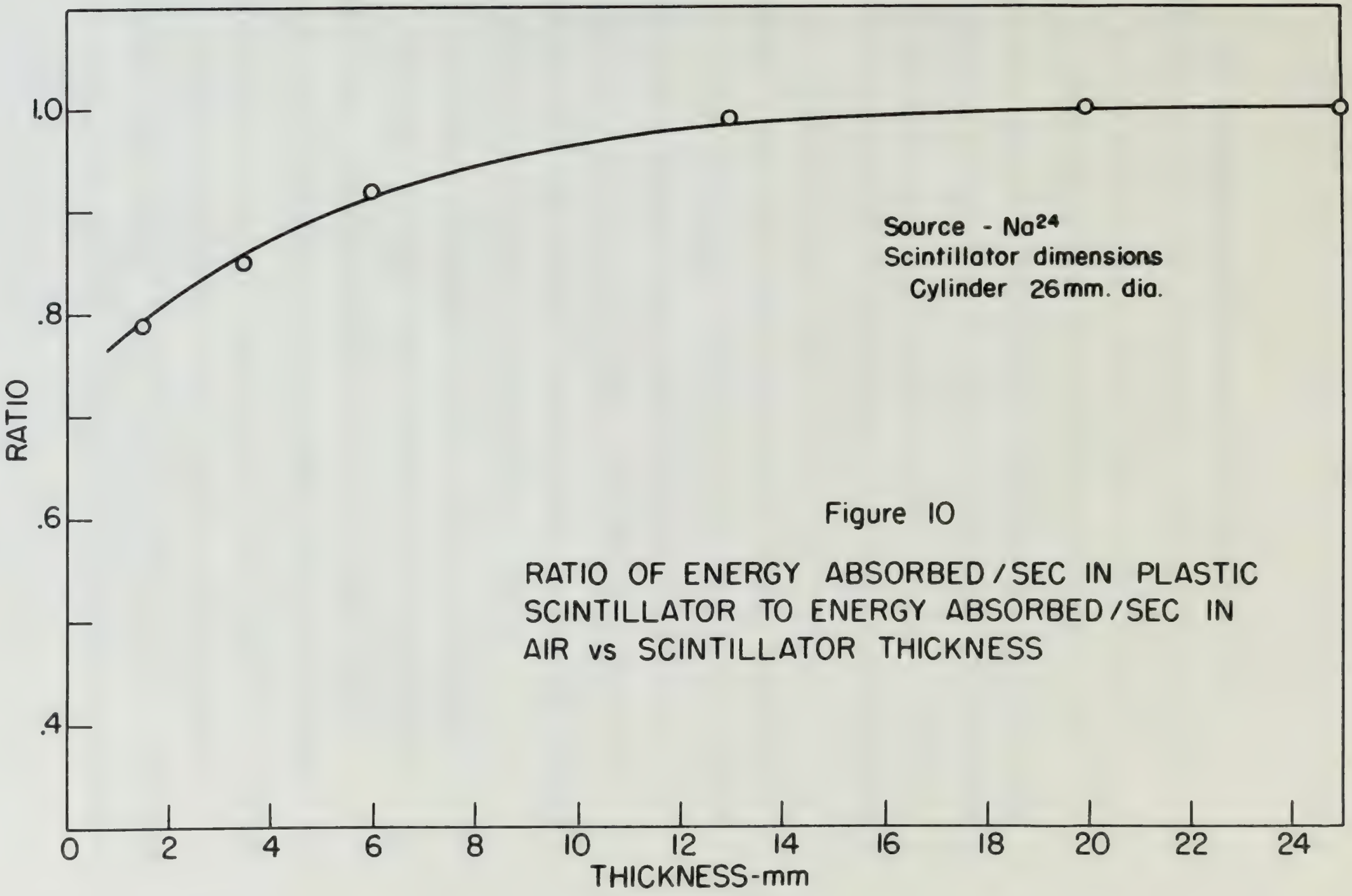

Source - Na^{24}
Scintillator dimensions
Cylinder 26mm. dia.

Figure 10

RATIO OF ENERGY ABSORBED / SEC IN PLASTIC SCINTILLATOR TO ENERGY ABSORBED / SEC IN AIR vs SCINTILLATOR THICKNESS

The measurements obtained using "broad beam" geometry and the 6 mm anthracene crystal are shown in Fig. 6. We observe that in the low energy region the experimental ratio lies below the theoretical. This is to be expected if scattered radiation is present since the average energy of the radiation reaching the detector would be lower than the average primary energy. At the average energy of Na^{24}, 2.07 Mev, the ratio is now closer to the theoretical than that obtained using "good" geometry. This can also be explained on the basis of a lowered average energy. Since for this thickness crystal experimental results show that little or no loss is expected for the average energy of Co^{60}, lowering the average energy of the Na^{24} source would reduce the effect of leakage loss thereby increasing the ratio.

The first indication of the effect of scattered radiation was apparent when a check of the ionization chamber for equilibrium conditions was made. Using "broad beam" geometry the front wall thickness of the ionization chamber was increased for four different sources. These results are shown in Fig. 11, and Fig. 8, curve D. Note that for the Cs^{137}, Co^{60}, and Na^{24} there is a decrease in dose rate as the wall thickness is increased from zero,

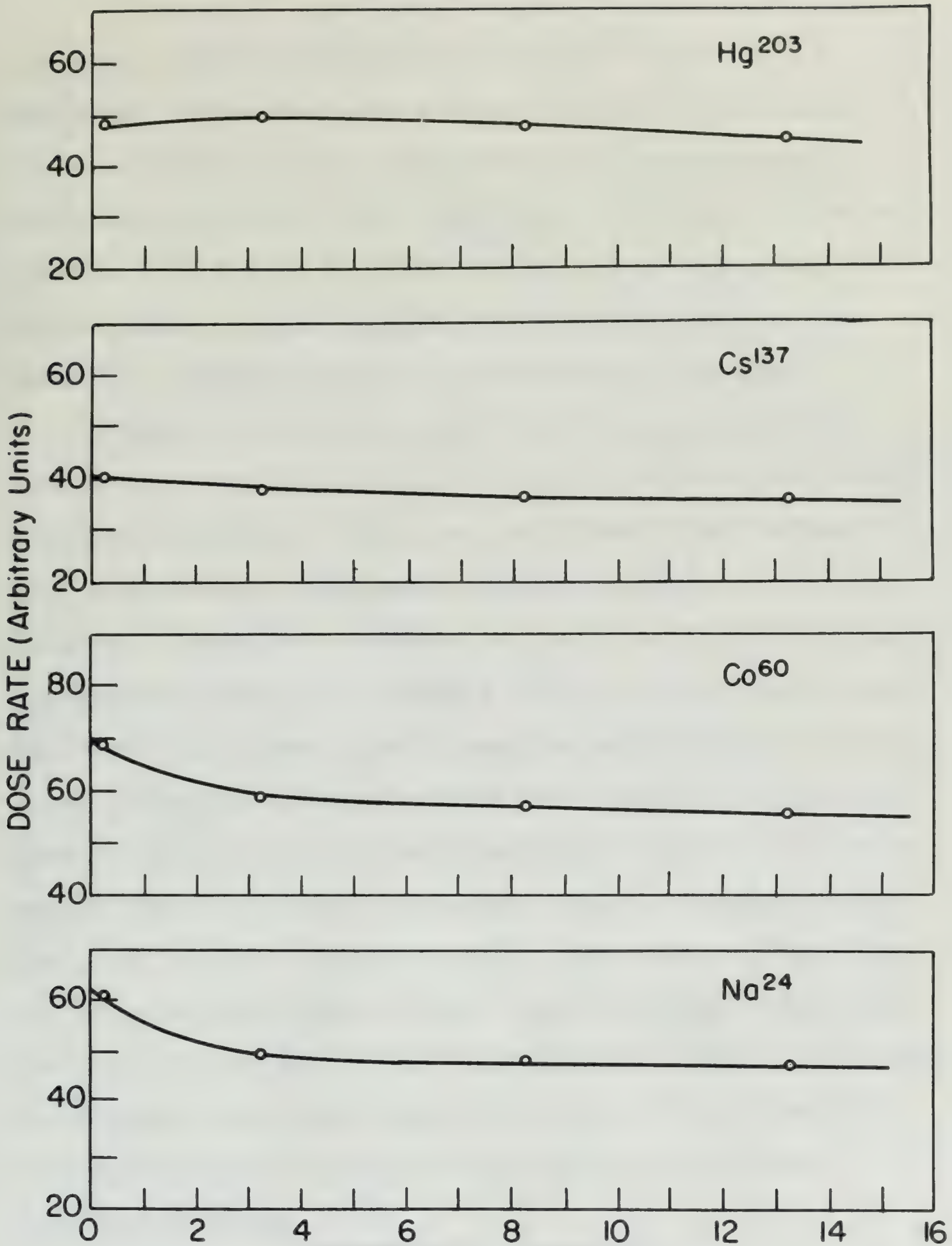

Figure 11

DOSE RATE vs FRONT WALL THICKNESS FOR AIR IONIZATION CHAMBER "BROAD" BEAM GEOMETRY

Source to chamber distance ~ 20 cm.

and only a slight build-up for the Hg^{203} source. To determine if the increase in dose rate was a function of the distance of the source over the range in which the measurements for this experiment were taken, three runs using a Na^{24} source at distances of 5 cm, 20 cm, and 50 cm were made. These results are shown in Fig. 12. No measurable difference due to distance was observed.

Further experimenting was undertaken by placing a lead sheet 8 inches square, 2 mm thick, between the source and the ion chamber. The lead was first placed adjacent to the source and then moved against the face of the ion chamber. Readings were taken for both positions and these are plotted in Fig. 8, curves B and C, for comparison with the "broad beam" and "good" geometry curves which are also shown in Fig. 8. With the lead sheet adjacent to the ion chamber some of the scattered radiation which is of lower energy than the primary radiation will be absorbed in the lead and, as the experiment shows, the curve for this condition approaches that for the "good" geometry. With the lead adjacent to the source none of the scattered radiation is attenuated and the curve is the same as that for the "broad beam" case except for some attenuation of the primary radiation.

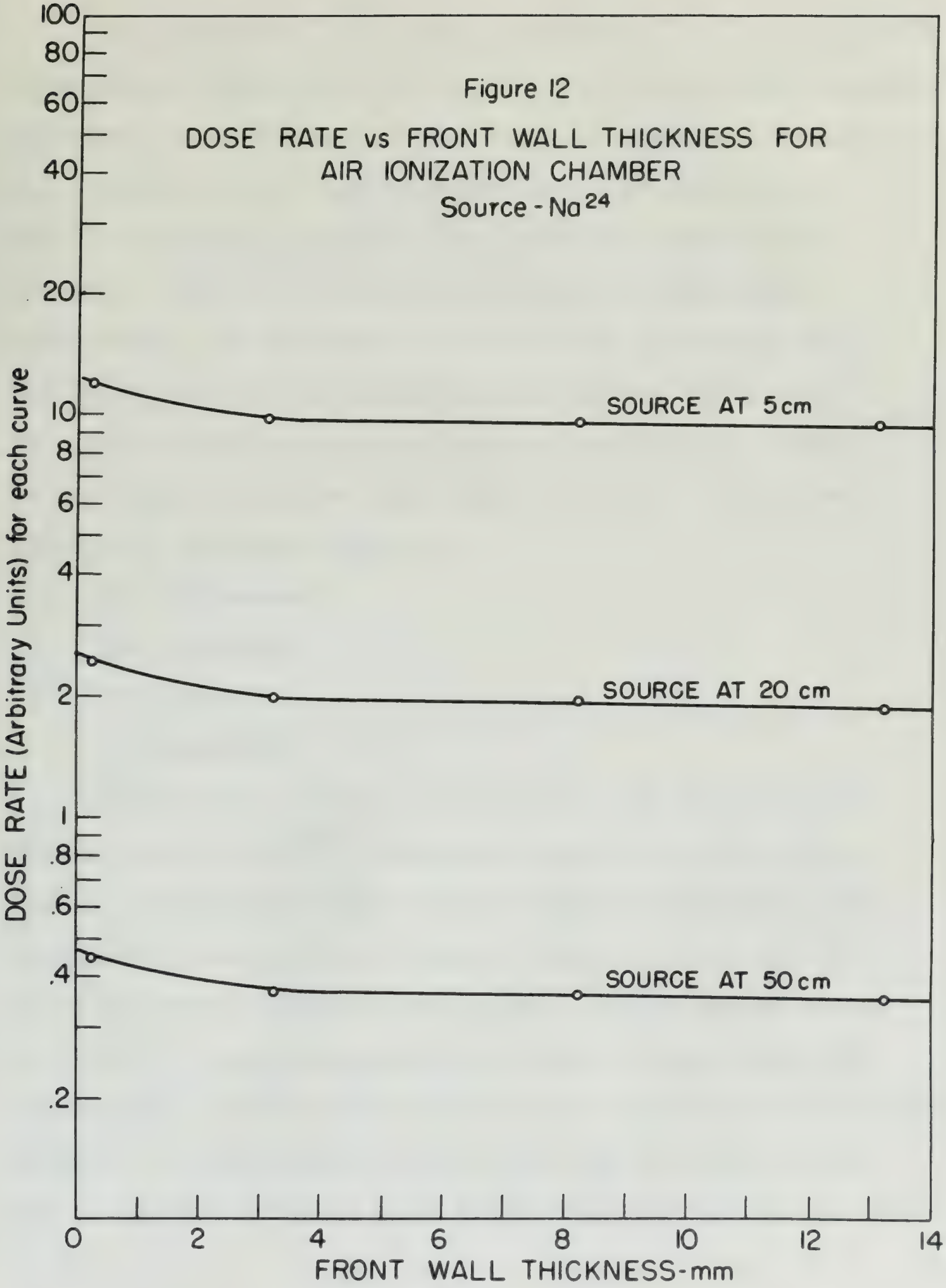

Figure 12

DOSE RATE vs FRONT WALL THICKNESS FOR AIR IONIZATION CHAMBER

Source - Na^{24}

In view of the probable applications of a scintillation dosimeter, measurements were made using "broad beam" geometry on several different types and sizes of organic scintillators. The results of these measurements are shown in Fig. 13. All of the organic scintillators used have essentially the same γ-ray attenuation coefficients as those for anthracene. An estimate of the relative efficiency of the different scintillators was made on the basis that the light output is directly proportional to the volume of the scintillator and the results in order of decreasing efficiency are given below:

1. Anthracene.
2. Stilbene.
3. Plastic
4. Terphenyl

Examination of Fig. 13 shows that the experimental results using an Hg^{203} source are always below the predicted theoretical curves and as previously mentioned this is probably a result of a lowered average energy due to the presence of scattered radiation. At the higher energy of the Na^{24} source examination of Fig. 13 shows that the experimental results also lie below the predicted theoretical curves. The experimental values for the thicker crystals are in closer agreement with theory than the values for the

Figure 13

RATIO OF ENERGY ABSORBED/SEC IN VARIOUS ORGANIC SCINTILLATORS TO ENERGY ABSORBED/SEC IN AIR vs INCIDENT GAMMA-RAY ENERGY

Note: All theoretical curves normalized to 0.6 Mev. — o

All experimental data normalized relative to Cs^{137} measurement — Δ

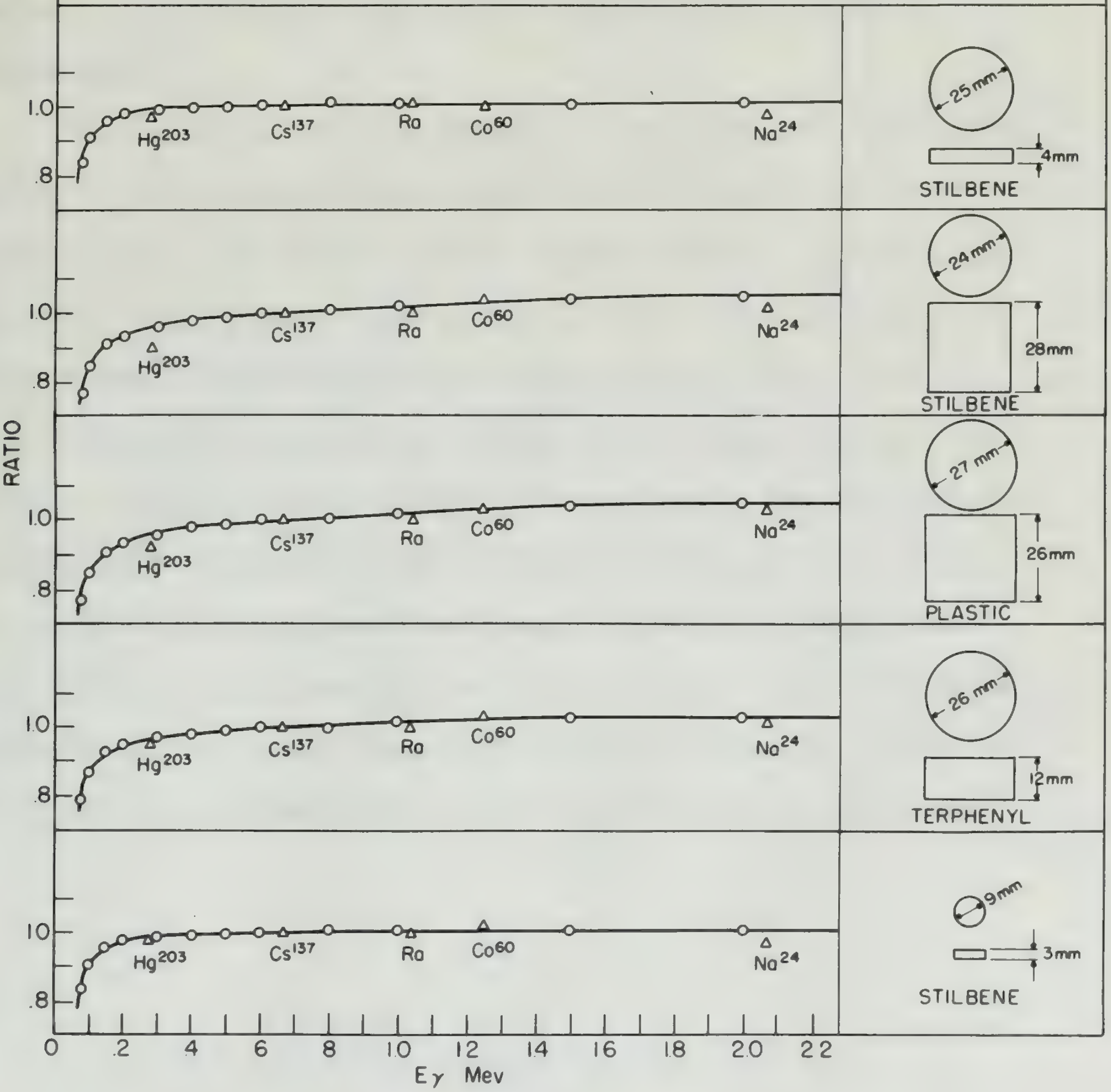

thinner crystals as would be expected if this decrease is due to leakage loss as explained in Section II-D.

All of the results, with the exceptions explained above, are seen to be in fairly close agreement with theory and it is therefore concluded that any of these organic scintillators would be suitable for use in a dosimeter.

To complete the experiment, measurements were taken using a NaI crystal which according to theory is "air-equivalent" over only a small energy range. The results of these measurements are shown in Fig. 14. Over the approximate "air-equivalent" range, which for a 25 mm NaI crystal is 0.5 Mev to 3 Mev, we see that the experimental results are in close agreement with the predicted theoretical values. Below 0.5 Mev the theoretical ratio is seen to increase as the energy decreases, therefore for "broad beam" geometry we would expect the experimental results to be higher than the predicted values. Examination of Fig. 14 shows that the results are as expected.

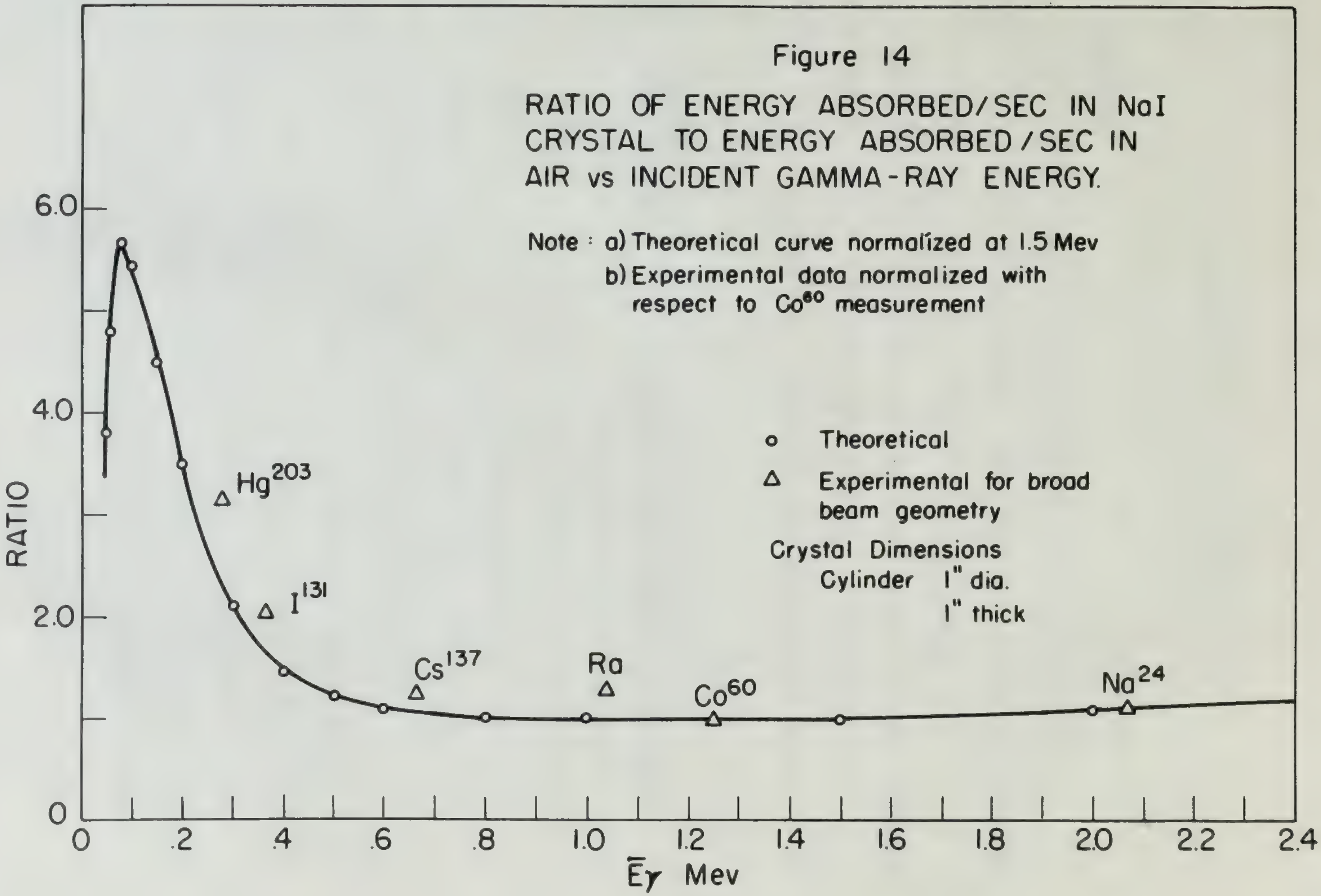

Figure 14

RATIO OF ENERGY ABSORBED/SEC IN NaI CRYSTAL TO ENERGY ABSORBED/SEC IN AIR vs INCIDENT GAMMA-RAY ENERGY.

Note : a) Theoretical curve normalized at 1.5 Mev
b) Experimental data normalized with respect to Co^{60} measurement

V. SUMMARY AND RECOMMENDATIONS

A. Summary

From the theoretical discussion in Section II and from the detailed experimental results described in Section IV the following general conclusions are made:

1. Organic scintillators are "air-equivalent" within ± 5 percent over a limited energy range depending on scintillator thickness as shown in the following table (see Fig. 4):

Scintillator thickness	Energy range for "air-equivalence" ± 5 percent
3 mm	0.12 Mev to ~7.0 Mev
6 mm	0.13 Mev to ~9.0 Mev
12 mm	0.20 Mev to >10 Mev
25 mm	0.25 Mev to >10 Mev

This table is based on a calibration of the scintillator at 0.8 Mev under equilibrium conditions.

2. When electronic equilibrium does not exist the "air-equivalent" range of the thinner scintillators will be considerably reduced from the values given in the above table as a result of leakage of secondary electrons from the sides of the scintillator.

3. There is no essential difference between the organic scintillators listed below in their response to γ radiation. They do, however, have different relative efficiencies for light output for the same incident radiation intensity. They are listed in order of decreasing efficiency.

a. Anthracene.

b. Stilbene.

c. Plastic.

d. Terphenyl.

4. Sodium iodide scintillation crystals are "air-equivalent" over a very limited energy range. They would therefore not be suitable for use in a scintillation dosimeter except in the measurement of dose rate from sources whose γ-ray spectrum lies completely in this range.

5. The effect of scattered radiation must be considered when using a scintillation dosimeter with "broad beam" geometry. Scattered radiation will lower the measurement at the low energy end of the "air-equivalent" range. The effect at the high energy end of the "air-equivalent" range will depend on the crystal thickness and on the thickness of material, if any, surrounding the crystal.

6. A scintillation dosimeter calibrated with a standard radium source will measure approximately 2.5

percent low for monoenergetic sources whose energies lie in the "air-equivalent" range.

B. Recommendations

It is recommended that a scintillation dosimeter be constructed similar to the one described in this experiment with the following modifications:

1. A cylindrical organic scintillator approximately 1/8 inch diameter, 3/8 inch thick mounted on the end of a lucite or quartz light pipe at least 1 foot long.

2. The scintillator encased in 3 mm of "air-equivalent" material such as bakelite.

3. Calibrated using a standard radium source.

The following investigations should then be conducted:

1. Investigate the effects of the light pipe.

2. Compare the results obtained in different phantoms when using the scintillation dosimeter with the results for the same phantoms when using a small air ionization chamber such as the Victoreen meter.

The results obtained from such an investigation would be invaluable to radiobiological research.

C. Conclusion

It is the belief of the author that the results of this investigation have shown beyond question the practicability of scintillation dosimeters for use in γ-ray measurements and it is hoped that application of such instruments will be of some value in future biological research.

APPENDIX A

SAMPLE CALCULATIONS

1. Calculation of μ_o/ρ, μ_a/ρ.

The values of μ_o/ρ and μ_a/ρ for air and NaI were obtained from the tables in NBS Report 1003.(15) For anthracene the values are not tabulated and must be calculated from the values given for hydrogen and carbon using the following formula:

$$\mu_o/\rho = \frac{1}{W} \sum_i W_i \frac{N_o \, {}_a\mu_{o_i}}{A_i}$$

$$\mu_a/\rho = \frac{1}{W} \sum_i W_i \frac{N_o \, {}_a\mu_{a_i}}{A_i}$$

where

W = molecular weight of compound

W_i = molecular weight of i'th element

A_i = atomic weight of i'th element

N_o = Avogadro's number

${}_a\mu_{o_i}$ = total attenuation cross section for i'th element

${}_a\mu_{o_i} = Z_i({}_e\sigma) + \tau + \kappa$

${}_a\mu_{a_i}$ = total absorption cross section for i'th element

${}_a\mu_{a_i} = Z_i({}_e\sigma_a) + \tau + \kappa$

For anthracene - $C_{14}H_{10}$ - with $E_\gamma = 1.0$ Mev

$$\tau_{\text{hydrogen}} = 0$$

$$\kappa_{\text{hydrogen}} = 0$$

$$Z_H({}_e\sigma_a)_{\text{hydrogen}} = 0.0929 \times 10^{-24}\ \text{cm}^2/\text{atom}$$

$$Z_H({}_e\sigma)_{\text{hydrogen}} = 0.2112 \times 10^{-24}\ \text{cm}^2/\text{atom}$$

$$({}_a\mu_o)_{\text{hydrogen}} = 0.2112 \times 10^{-24}\ \text{cm}^2/\text{atom}$$

$$({}_a\mu_a)_{\text{hydrogen}} = 0.0929 \times 10^{-24}\ \text{cm}^2/\text{atom}$$

$$\tau_{\text{carbon}} = 0$$

$$\kappa_{\text{carbon}} = 0$$

$$Z_C({}_e\sigma_a)_{\text{carbon}} = 0.5574\ \text{cm}^2/\text{atom}$$

$$Z_C({}_e\sigma)_{\text{carbon}} = 1.267\ \text{cm}^2/\text{atom}$$

$$({}_a\mu_o)_{\text{carbon}} = 1.267\ \text{cm}^2/\text{atom}$$

$$({}_a\mu_a)_{\text{carbon}} = 0.5574\ \text{cm}^2/\text{atom}$$

$$W_{\text{carbon}} = 168\ \text{gm/mole}$$

$$W_{\text{hydrogen}} = 10\ \text{gm/mole}$$

$$W = 178\ \text{gm/mole}$$

$$N_o = 6.03 \times 10^{23}\ \text{atoms/gm-mole}$$

$$\frac{\mu_o}{\rho} = \frac{1}{178} \sum \frac{(10)(6.03 \times 10^{23})(0.2112 \times 10^{-24})}{1} +$$

$$+ \frac{168(6.03 \times 10^{23})(1.267 \times 10^{-24})}{12}$$

$$\frac{\mu_o}{\rho} = 0.0671 \text{ gm/cm}^2$$

Similarly

$$\frac{\mu_a}{\rho} = 0.0295 \text{ gm/cm}^2$$

2. Calculation of ratio R for anthracene crystal 24 mm thick and $E_\gamma = 1.0$ Mev

$$R = C\frac{\mu_a}{\mu_a{}'}\left(\frac{1 - e^{-\mu_o}}{\mu_o}\right)$$

$$\frac{\mu_a}{\rho} = 0.0295 \text{ gm/cm}^2$$

$$\frac{\mu_o}{\rho} = 0.0671 \text{ gm/cm}^2$$

$$\frac{\mu_a{}'}{\rho'} = 0.0279 \text{ gm/cm}^2$$

$\rho = 1.25 \text{ gm/cm}^3$ density of anthracene

$\rho' = 0.001205 \text{ gm/cm}^3$ density of dry air 20°C and 760 mm

$$R_{1.0} = \frac{C(1.25)(0.0295)}{(0.001205)(0.0279)}\left(\frac{1 - e^{-(1.25)(0.0671)(2.4)}}{(1.25)(0.0671)(2.4)}\right)$$

$$R_{1.0} = 985.1 \text{ C}$$

From similar calculation for $E_\gamma = 0.6$ Mev

$$R_{0.6} = 964.7\ C$$

Normalizing at 0.6 Mev let $C = \frac{1}{964.7}$, then $(R_{0.6})_{norm} = 1$

and the normalized value of $R_{1.0}$ becomes

$$(R_{1.0})_{norm} = \frac{985.1}{964.7} = 1.01$$

3. Calculation of $\overline{E_\gamma}$

Na^{24} has two γ rays

E_γ	Percent abundance
1.38 Mev	100
2.76 Mev	100

$$\overline{E_\gamma} = \sum_i P_i E_{\gamma_i} / \sum P_i$$

$$\overline{E_\gamma} = \frac{100(1.38) + 100(2.76)}{200} = 2.07 \text{ Mev}$$

4. Calculation of ratio R for non-monoenergetic source using exact formula compared with calculation of R using $\overline{E_\gamma}$

$$R_{\sum_i} = \frac{C \sum_i n_{o_i} E_{\gamma_i} \mu_{a_i} \left[\frac{1 - e^{-\mu_{o_i} \ell}}{\mu_{o_i} \ell} \right]}{\sum_i n_{o_i} E_{\gamma_i} \mu_a{}'_i}$$

For Na^{24} considering ratio of anthracene to air

		Anthracene		Air
		μ_a/ρ	μ/ρ	μ_a'/ρ'
$E_{\gamma 1}$	1.38 Mev	0.029	0.060	0.026
$E_{\gamma 2}$	2.76 Mev	0.024	0.041	0.021
$\overline{E_\gamma}$	2.07 Mev	0.026	0.048	0.023

For non-monoenergetic with d = 6 mm

$$n_{o_1} = n_{o_2}$$

$$R_{\sum_i} = \frac{C(0.029)(1.38)(1.25)\left(\frac{1 - e^{-(0.06)(0.6)(1.25)}}{(0.06)(0.6)(1.25)}\right)}{0.001205\ (0.026)(1.38) + (0.021)(2.76)} +$$

$$+ \frac{C(0.024)(2.76)(1.25)\left(\frac{1 - e^{-(0.041)(0.6)(1.25)}}{(0.041)(0.6)(1.25)}\right)}{0.001205\ (0.026)(1.38) + (0.021)(2.76)}$$

$$R_{\sum_i} = 1141\ C$$

For average energy

$$R_{\overline{E_\gamma}} = \frac{C(0.026)(1.25)\left(\frac{1 - e^{-(0.048)(0.6)(1.25)}}{(0.048)(0.6)(1.25)}\right)}{0.001205(0.023)}$$

$$R_{\overline{E_\gamma}} = 1148\ C$$

Comparison of $R_{\sum_i}$ with $R_{\overline{E_\gamma}}$ shows that the error introduced by the use of $\overline{E_\gamma}$ is $\sim$ 0.6 percent.

BIBLIOGRAPHY

1. Ittner, W. B., III, and M. Ter-Pogossian: Nucleonics 10, No. 2, 48 (1952)
2. Brucker, G.J.: Nucleonics 10, No. 11, 72 (1952)
3. Prestwich, G. D. and T. H. Colvin: M.I.T. Thesis (1952)
4. Evans, R. D.: Nucleonics 1, No. 2, 32 (1947)
5. Gray, L. H.: Proc. Roy. Soc. (London) 156A, 578 (1936)
6. Gray, L. H.: Proc. Cambridge Phil. Soc. 40, 72 (1944)
7. Sangster, R. C.: O.N.R. Technical Report 55, 34 (1952)
8. Hopkins, J. I.: Rev. Sci. Instr. 22, 29 (1952)
9. Evans, R. D.: Revs. Modern Phys. 24, 79 (1952)
10. Gray, L. H.: Brit. J. Radiol. 10, 600, 721 (1937)
11. Mayneord, W. V. and J. E. Roberts: Brit. J. Radiol. 10, 365 (1937)
12. Haskins, J. R. and J. D. Kurbatov: Phys. Rev. 88, 884 (1952)
13. Hine, G. J.: Phys. Rev. 82, 755 (1951)
14. Gray, L. H.: Proc. Roy. Soc. (London) 122A, 647 (1928)
15. White, G. R.: N.B.S. Report 1003 (1952)

JUL 2
JAN 29
AP 18 56

BINDERY
4186
4142

20655
Thesis Carr
C2715 Dosage measurements usin
organic scintillators.

JAN 29
AP 18 56

BINDERY
4186
4142

20655
Thesis Carr
C2715 Dosage measurements using organic scintillators.

Library
U. S. Naval Postgraduate School
Monterey, California

ARTISAN
GOLD LETTERING
AND
SMITH BINDERY
OAKLAND, CALIF.

thesC2715
Dosage measurements using organic scinti
3 2768 002 09239 7
DUDLEY KNOX LIBRARY